Available online at www.sciencedirect.com
SCIENCE DIRECT®
Hearing Research 177 (2003) 61–70
HEARING RESEARCH
www.elsevier.com/locate/heares

Relationship between the local stiffness of the outer hair cell along the cell axis and its ultrastructure observed by atomic force microscopy

Hiroshi Wada [a,*], Hiroto Usukura [a], Michiko Sugawara [a], Yukio Katori [b], Seiji Kakehata [c], Katsuhisa Ikeda [b], Toshimitsu Kobayashi [b]

[a] *Department of Mechanical Engineering, Tohoku University, Aoba-yama 01, Sendai 980-8579, Japan*
[b] *Department of Otorhinolaryngology – Head and Neck Surgery, Tohoku University Graduate School of Medicine, Sendai, Japan*
[c] *Department of Otorhinolaryngology, Hirosaki University School of Medicine, Hirosaki, Japan*

Received 1 May 2002; accepted 20 December 2002

Abstract

As electromotility may arise from a conformational change of the molecules' 'protein motors', which might be distributed along the outer hair cell (OHC) lateral wall, the force generated by the OHC electromotility would be related not only to the conformational change of the protein motors but also to the mechanical properties of the lateral wall. Therefore, a detailed understanding of the mechanical properties of the OHC lateral wall is important. In our previous reports, to understand the difference in the stiffness along the cell axis, the local deformation of the OHC in response to hypotonic stimulation was analyzed by measuring the displacement of microspheres attached randomly to the cell lateral wall, and the distribution of Young's modulus along the cell axis was obtained using the contact mode of an atomic force microscope (AFM). These investigations revealed that the stiffness of the cell in the apical region was greater than that in other regions where the stiffness is constant. In this study, the ultrastructure of the OHC lateral wall was investigated with the oscillation imaging mode of the AFM (Tapping Mode™), and the relationship between the stiffness along the cell axis and the ultrastructure that was observed by the AFM imaging was analyzed. From the analysis, it was concluded that the circumferential filaments observed in the tapping mode AFM are actins which are part of the cortical lattice, and that the difference between the intervals of the circumferential filaments in the apical region and those in other regions is one factor that causes the high stiffness in the apical region.

Key words: Ultrastructure; Outer hair cell; Lateral wall; Cortical lattice; Actin filament; Atomic force microscopy

1. Introduction

The outer hair cell (OHC) is cylindrical in shape with a radius of 4–5 μm and a length of 30–90 μm. It is capped by the cuticular plate with stereocilia at the apical end and by the synaptic membrane at the basal end. As the cuticular plate is composed of a dense network of actin filaments, it is considered to be rigid. The OHC lateral wall consists of three layers: the plasma membrane, the cortical lattice and the subsurface cisternae. The cortical lattice is located between the plasma membrane and the subsurface cisternae and may function to maintain cell shape. The cortical lattice consists of two types of filaments: actin and spectrin (Holley and Ashmore, 1990a). From electron microscopic studies, it has been demonstrated that actins, which are arranged circumferentially, are 5–8 nm in diameter and are cross-linked at regular intervals by thinner spectrins, 2–4 nm in diameter (Holley and Ashmore, 1988, 1990a,b; Holley et al., 1992; Arima et al., 1991). The outermost plasma membrane is likely to be linked to the cortical lattice by the pillars and contains a high density of membrane particles (Arima et al., 1991; Forge, 1991; Kalinec et al., 1992). The innermost subsurface cisternae are known to be much softer than the plasma membrane.

* Corresponding author: Tel.: +81 (22) 217-6938; Fax: +81 (22) 217-6939.
E-mail address: wada@cc.mech.tohoku.ac.jp (H. Wada).

0378-5955/03/$ – see front matter © 2003 Elsevier Science B.V. All rights reserved.
doi:10.1016/S0378-5955(02)00798-0

It has been thought that the motility of the OHC results from conformational changes of protein motors. From microscopic studies of the cell lateral wall, membrane particles are known to be present in the plasma membrane (Arima et al., 1991; Forge, 1991; Kalinec et al., 1992). When the cortical lattice and the subsurface cisternae were disrupted by intracellular trypsin digestion and only the plasma membrane remained, the OHC was still motile (Kalinec et al., 1992; Huang and Santos-Sacchi, 1994). Moreover, the existence of a nonlinear gating charge movement or a nonlinear capacitance (Santos-Sacchi, 1991) was clarified by a whole-cell patch-pipette recording. Therefore, the particles that are distributed along the plasma membrane are protein motor candidates. Recently, Zheng et al. (2000) identified the gene that encodes a specialized motor protein that produces the motility and designated it 'prestin'. When prestin was expressed in cultured human kidney cells, the cells showed a motile response and nonlinear capacitance (Zheng et al., 2000). Therefore, prestin is a motor protein which may be distributed along the lateral wall of the OHC.

To evaluate the OHC's ability to influence basilar membrane motion and tuning, the mechanical properties of the OHC lateral wall should be ascertained in advance, because the force produced by the elongation and contraction of the OHC is influenced by the mechanical properties of the OHC lateral wall. It has been reported that the longitudinal whole cell stiffness was found to be in the range of 0.8–25 mN/m (Zenner et al., 1992; Hallworth, 1995) from the length change of the OHC in response to an external stimulus. However, as there is a structural difference between the apical part that has the cuticular plate and the basal part that has a half-spherical shape, it is possible that the local stiffness in a specific region of the OHC lateral wall is different from that in the other regions.

In our previous paper (Wada et al., 2001), to understand the difference in the stiffness along the cell axis, the local deformation of the OHC in response to hypotonic stimulation was analyzed by measuring the displacement of microspheres attached randomly to the cell lateral wall. The investigation revealed that the stiffness of the cell was constant in the region between 0.0 and 0.88 while that in the region between 0.88 and 1.0 it was higher than in other regions, where the position along the cell axis was represented by the normalized distance from the basal end and the positions of the basal and apical ends were expressed by 0.0 and 1.0, respectively. In addition, Sugawara et al. (2002) reported that Young's moduli in the apical region of the OHC were larger than those in the middle and basal regions using the contact mode of an atomic force microscope (AFM). In this study, the ultrastructure of the OHC lateral wall was investigated under nearly physiological conditions using the oscillation imaging mode of the AFM (Tapping Mode™, Digital Instruments, Santa Barbara, CA, USA), and the relationship between the stiffness along the cell axis and the ultrastructure that was observed by the AFM imaging was analyzed.

2. Materials and methods

2.1. Cell preparation

Guinea pigs weighing 200–300 g were used. They were decapitated and the temporal bones were removed. After opening the bulla, the cochlea was detached and transferred to an experimental bath (the major ions in the medium were NaCl, 140 mM; KCl, 5 mM; $CaCl_2$, 1.5 mM; $MgCl_2{\cdot}6H_2O$, 1.5 mM; HEPES, 5 mM; glucose, 5 mM; pH 7.2; 300 mOsm). The bony shell covering the cochlea was removed and the apical and middle two turns of the organ of Corti were gently scraped off from the basilar membrane. After enzymatic incubation with dispase (500 PU/ml), the OHCs were isolated by gently pipetting the organ of Corti in the experimental bath. The isolated OHCs were transferred to a chamber and fixed in 2.5% glutaraldehyde in 0.1 M phosphate buffer for 30 min at room temperature. After fixation, the OHCs were washed in an experimental bath.

Care and use of animals reported in this study were approved by the Institutional Animal Care and Use Committee of Tohoku University, Sendai, Japan.

2.2. Light microscopy

In order to investigate cell length change due to fixation, the OHCs were observed with an inverted microscope (IX50, Olympus) and images of the cells were acquired with a CCD camera system (CS5110C, Tokyo Electronic Industry). Then, images were analyzed offline using a personal computer. One pixel in the recorded digital picture from the CCD camera corresponded to 240 nm, and each pixel was quantified using a gray scale of 256. From acquired images, lengths of the isolated OHC before and after fixation were analyzed.

2.3. Atomic force microscopy

Images of the OHC lateral wall were recorded in the experimental bath with an AFM (NVB100, Olympus). The AFM was mounted on an inverted microscope. V-shaped silicon nitride cantilevers and pyramidal tips (OMCL-TR400PSA-2, Olympus) were used. The spring constant of the cantilever was 0.08 N/m and the tip's typical radius of curvature was less than 20 nm. In this

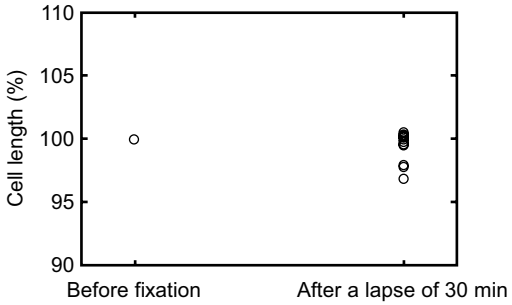

Fig. 1. Change in cell length during cell fixation. The ordinate shows the cell length divided by the initial cell length in percent. OHCs were fixed with 2.5% glutaraldehyde in 0.1 M phosphate buffer. The number of measured OHCs was 14.

experiment, tapping mode AFM was used under fluid. In the tapping mode AFM, the tip was oscillated with high frequency in the vertical direction and was only intermittently in contact with the sample. In this study, the scanning region was 1 μm × 2 μm or 0.5 μm × 1 μm, and the scanning frequency was 0.5 Hz (scan speed: 1.00 μm/s) or 0.389 Hz (scan speed: 0.389 μm/s), respectively. In all AFM images, the sample was scanned from left to right. The scanning direction corresponds to the axial direction of the OHC. The images obtained by the measurement from the AFM were analyzed by software provided by Digital Instruments. The correction of the images by this software enabled reduction of the noise. Application of section analysis to the features of the images made it possible to measure the size or distance of the surface features.

3. Results

Length change of the OHCs during cell fixation was measured. Fig. 1 shows change in cell length when the OHCs were fixed with 2.5% glutaraldehyde in 0.1 M phosphate buffer. The ordinate shows the cell length divided by the initial cell length in percent. From this result, the mean value of the cell length after fixation was 99.5 ± 1.1% ($n = 14$).

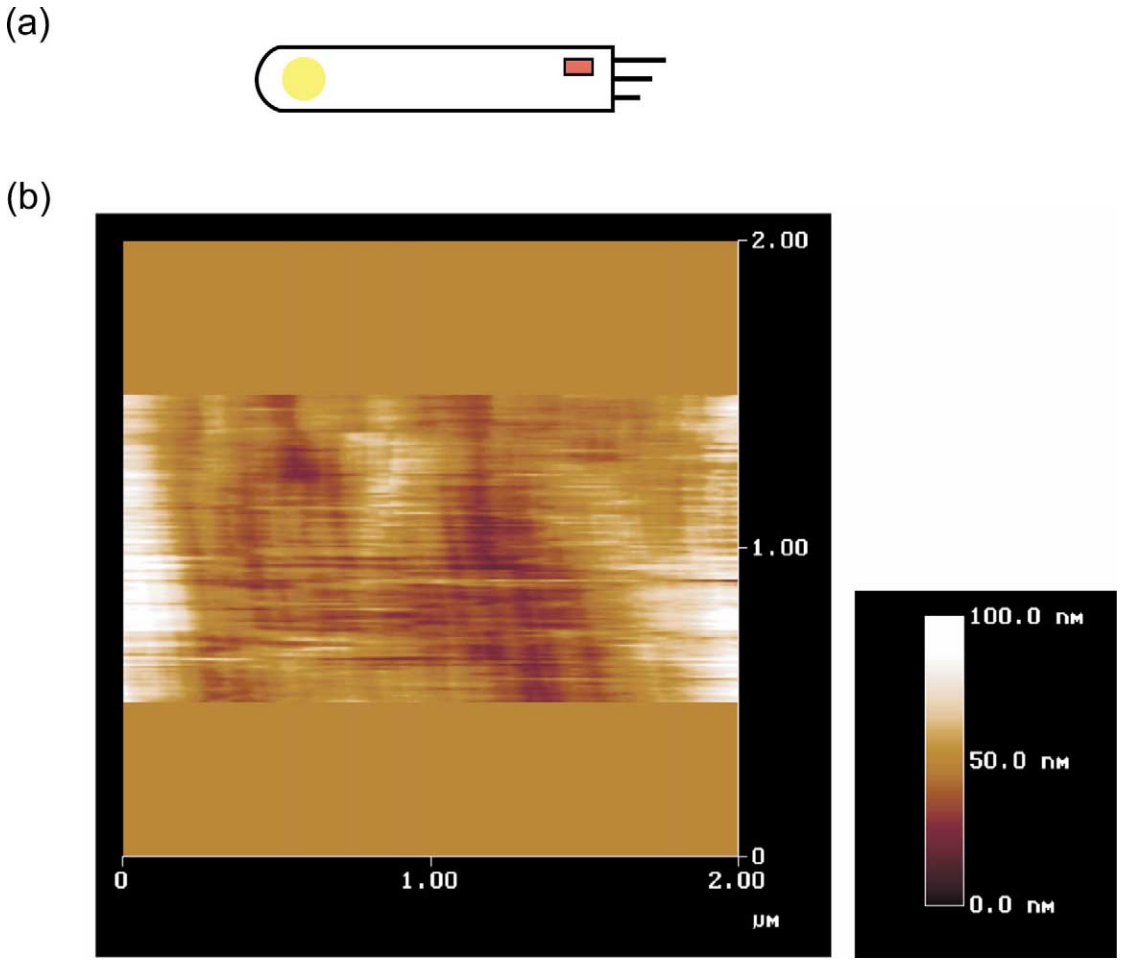

Fig. 2. AFM image of the lateral surface in the apical region of the OHC. (a) The position of the scanning area. The ultrastructure in the red area in this figure was measured by AFM. (b) The AFM image obtained by scanning the red area in panel a. The scanning area and frequency are 1 μm × 2 μm and 0.5 Hz, respectively. The filaments can be clearly seen and are arranged in the circumferential direction of the cell.

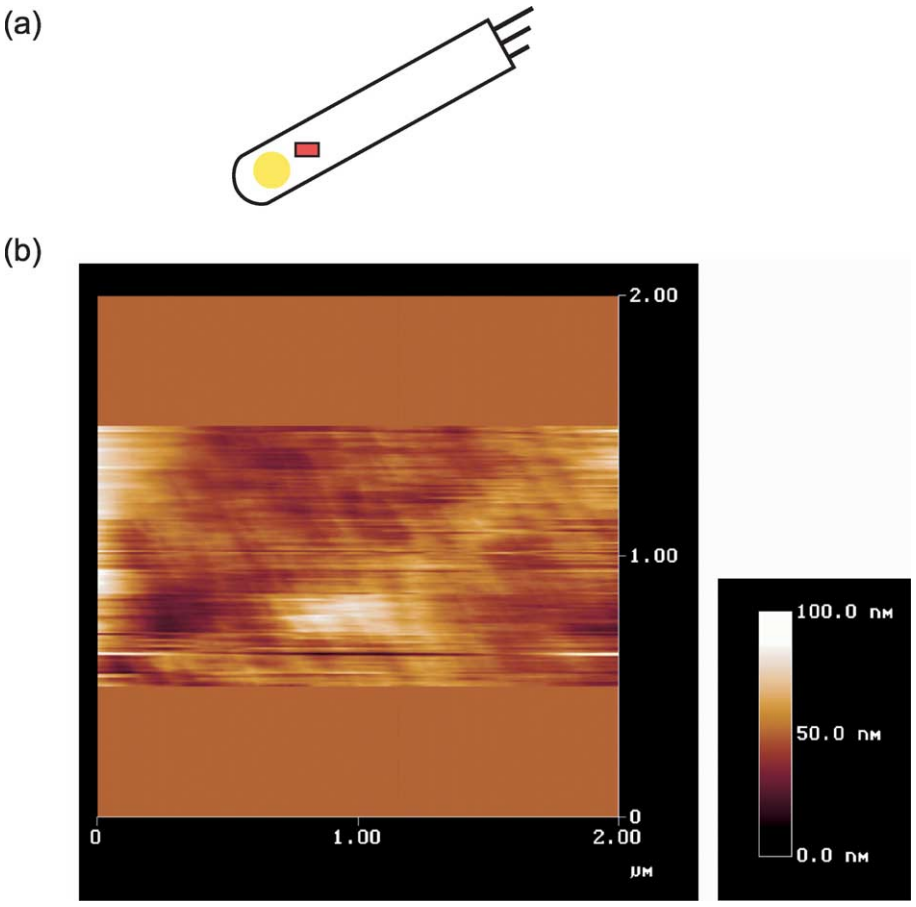

Fig. 3. AFM image of the lateral surface in the middle region of the OHC. (a) The position of the scanning area. The scan angle is different from that in Fig. 2. (b) The AFM image obtained by scanning the red area in panel a. The scanning area and frequency are 1 μm×2 μm and 0.5 Hz, respectively. Again, the filaments can be clearly seen and are arranged in the circumferential direction of the cell.

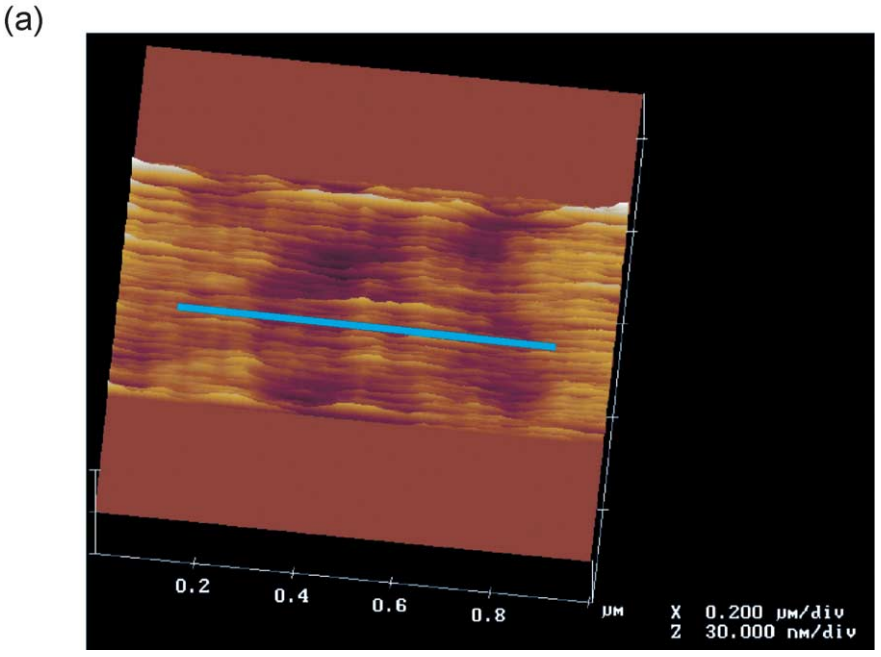

Fig. 4.

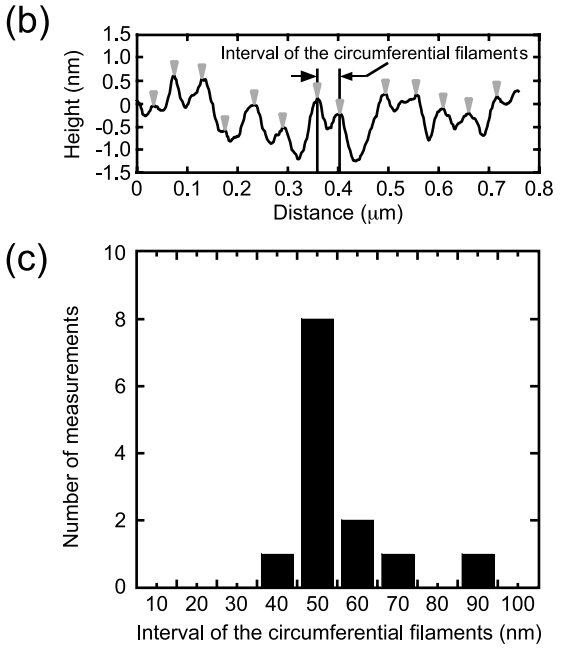

Fig. 4 (*Continued*). Section analysis. (a) AFM image of the circumferential filaments. The scanning area and frequency are 0.5 μm×1 μm and 0.389 Hz, respectively. (b) The surface profile along the blue line shown in panel a. The image was sectioned along the blue line, which is orthogonal to the direction of the filaments. The intervals of peak values of the surface profile which are shown by blue arrowheads are considered to be those of the circumferential filaments. (c) The number of measurements versus intervals of the circumferential filaments in panel b. The number of measurements is plotted against the 10 nm class intervals. The intervals range from 41 nm to 90 nm and their mean and the standard deviation are 58 nm and 12 nm, respectively.

The lateral surface of the fixed OHC was scanned using the tapping mode AFM. Fig. 2 shows the image obtained in the apical region of the OHC. The position of the scanning area is shown in Fig. 2a, and the image is shown in Fig. 2b. The scanning area and frequency were 1 μm×2 μm and 0.5 Hz, respectively. In this image, the circumferentially arranged filaments were discerned. Fig. 3 shows the image obtained in the middle region of the OHC. As illustrated in Fig. 3a, the image shown in Fig. 3b was obtained with a scan angle which was different from that of Fig. 2. From this image, the circumferentially arranged filaments were also discerned. These filaments were also seen in the images obtained in the other regions of the OHC, and all of them were arranged circumferentially. To evaluate the circumferential filaments, their intervals were measured by section analysis. In this analysis, the image of a 0.5 μm×1 μm scanning area with a scanning frequency of 0.389 Hz was sectioned along a line orthogonal to the direction of the filaments (Fig. 4a) and the surface profile of the section was plotted (Fig. 4b). From this surface profile, the intervals of its peak values shown by blue arrowheads in Fig. 4b were considered to be those of the circumferential filaments. Fig. 4c shows the number of measurements plotted against the 10 nm class intervals, which was determined from Fig. 4b. The intervals of the circumferential filaments ranged from 41 nm to 90 nm, and the mean and their standard deviations were 58 nm and 12 nm, respectively. The 38 images obtained from 13 OHCs with the scanning area of 0.5 μm×1 μm and the scanning frequency of 0.389 Hz were analyzed in the region between 0.1 and 0.98 from the basal end, where the position along the cell axis was represented by the normalized distance from the basal end and the positions of the basal and apical ends were expressed by 0.0 and 1.0, respectively. Fig. 5 shows the number of measurements plotted against the 10 nm class intervals. The intervals ranged from 15 nm to 103 nm, and the mean and their standard deviations were 49 nm and 18 nm, respectively.

4. Discussion

4.1. Effect of fixation on the cell length

In this study, as the living OHC was too soft for AFM observation and the cell lateral wall could not be visualized under physiological conditions, the OHC was fixed with glutaraldehyde. Slepecky and Ulfendahl (1988) reported that glutaraldehyde induced shortening of OHCs and that length changes up to 10% of the total cell length were observed. In this study, however, when the effect of glutaraldehyde fixation on whole cell length

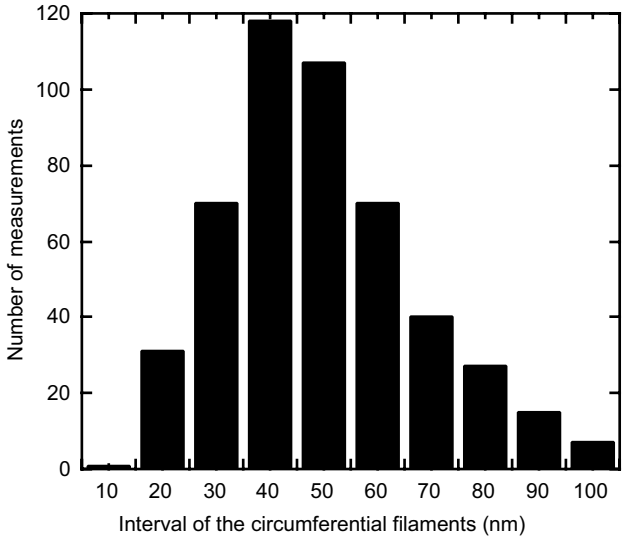

Fig. 5. The number of measurements versus intervals of the circumferential filaments. The intervals of the circumferential filaments in the 38 images range from 15 nm to 103 nm and their mean and the standard deviation are 49 nm and 18 nm, respectively.

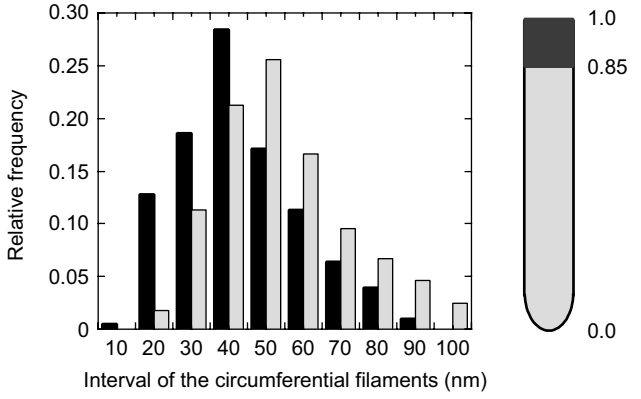

Fig. 6. The frequency of measurements versus intervals of the circumferential filaments in the apical region and that in the other region. The gray and black bars indicate the intervals of the circumferential filaments in the region between 0.0 and 0.85 and between 0.85 and 1.0 from the basal end, respectively. In order to allow direct comparison, the frequency of measurements in each class is plotted as the percentage of the total number of measurements against the 10 nm class intervals.

of OHCs was observed by an optical inverted microscope, the OHCs were shortened only $0.5 \pm 1.1\%$ ($n = 14$). Therefore, the OHCs were regarded to be fixed without deformation macroscopically.

4.2. Ultrastructure of the OHC lateral wall

When the lateral surface of the fixed OHC was scanned using tapping mode AFM, circumferential filaments were observed in every region of the OHC. Their intervals were 49 ± 18 nm with a range of 15–102 nm. Some studies have been reported in which the cytoskeleton network was observed in XR1, RBL-2H3 and SK-N-SH cells by AFM imaging of the periphery of a cell (Henderson et al., 1992; Chang et al., 1993; You et al., 2000). In electron microscopic studies on the OHC lateral wall, it has been demonstrated that the cortical lattice lies beneath the lateral plasma membrane along the full length of the cell and has actins that are arranged circumferentially (Holley and Ashmore, 1988, 1990a,b; Arima et al., 1991). Holley et al. (1992) reported that the mean interval of actins was 61.6 ± 8.0 nm with a range of 42–82 nm in the sectioned cells fixed without extraction. Additionally, in the negative stained cells, actin filaments with a mean interval of 56.2 ± 7.3 nm have been observed (Holley et al., 1992). As the direction, the distribution and the interval of these filaments are similar to our results, the filaments that were observed in the tapping mode AFM would be actin filaments that are part of the cortical lattice.

It has been reported that the filaments in the cortical lattice form discrete domains that are oriented at various angles to each other (Holley et al., 1992). In other words, although filaments run parallel to each other within a single domain, individual domains are arranged at different angles to the transverse axis of the cell. However, the domains were not clear in the present study. Spectrins cross-linking the actin filaments were also not observed in this study. One of the reasons for their absence is that spectrins are difficult to observe as they are thinner than the actins. Another reason is as follows: Leonova and Raphael (1999) reported that the spectrins constituted a thin flexible meshwork underlying the actins. If their model of the cortical lattice is correct, there is a possibility that only actins are scanned, because the actins and spectrins constitute different layers. Further study on this point is necessary for more detailed analysis.

Table 1
Interval of the circumferential filaments in the apical region and in the other region

Region (from the basal end)	Mean (nm)	S.D. (nm)	Minimum (nm)	Maximum (nm)	Number of measurements	Number of OHCs
Between 0.0 and 0.85	54	18	18	103	282	8
Between 0.85 and 1.0	44	17	15	97	204	7

The difference between the mean interval of the circumferential filaments in the region between 0.0 and 0.85 from the basal end and that in the region between 0.85 and 1.0 from the basal end was statistically significant at $P < 0.05$ using Student's t-test.

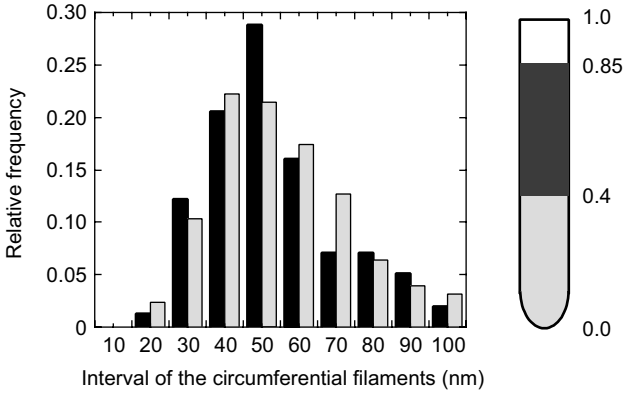

Fig. 7. The frequency of measurements versus intervals of the circumferential filaments in the middle and basal regions. The gray and black bars indicate the interval of the circumferential filaments in the region between 0.0 and 0.40 and between 0.40 and 0.85 from the basal end, respectively. In order to allow direct comparison, the frequency of measurements in each class is plotted as the percentage of the total number of measurements against the 10 nm class intervals.

4.3. Relationship between the local stiffness and the ultrastructure

In our previous paper (Wada et al., 2001), it was concluded that the longitudinal stiffness of the OHC in the region between 0.88 ± 0.045 and 1.0 from the basal end is greater than that in the other regions, where the position along the cell axis was represented by the normalized distance from the basal end and the positions of the basal and apical ends were expressed by 0.0 and 1.0, respectively. In addition, Sugawara et al. (2002) reported that Young's modulus in the apical region of the cell is a maximum of threefold larger than those in the middle and basal regions using the contact mode of the AFM. To discuss the relationship between the local stiffness and the ultrastructure, which was observed by AFM imaging, the intervals of the circumferential filaments were evaluated locally. The interval of the circumferential filaments in the region between 0.0 and 0.85 from the basal end and that in the region between 0.85 and 1.0 from the basal end are shown in Fig. 6. In this figure, to allow a direct comparison, the frequency of measurements in each class is plotted as the percentage of the total number of measurements against the 10 nm class intervals. The mean and standard deviation of the interval of the circumferential filaments in the region between 0.0 and 0.85 from the basal end and that in the region between 0.85 and 1.0 from the basal end were 54 ± 18 nm and 44 ± 17 nm, respectively (Table 1). The difference of these means was statistically significant at $P < 0.05$ using Student's t-test. On the other hand, as shown in Fig. 7 and Table 2, the mean and standard deviation of the interval of the circumferential filaments in the region between 0.0 and 0.4 from the basal end and that in the region between 0.4 and 0.85 from the basal end were identical, namely, 54 ± 18 nm and 54 ± 17 nm, respectively. These results show that the intervals of the circumferential filaments in the region between 0.85 and 1.0 from the basal end are narrower than those in the region between 0.0 and 0.85 from the basal end.

The relationship between the intervals of the circumferential filaments and the longitudinal stiffness of the OHC lateral wall is evaluated as follows. When the OHC is perfused with hypotonic solution, the longitudinal force F and circumferential force $2F$ induced by the increase in the intracellular pressure act on the lateral wall of the cell (Fig. 8). Applying the membrane theory, Hook's law and the principle of superposition to this model, the longitudinal strain ε_x and circumferential strain ε_θ of the cell lateral wall are given by

$$\varepsilon_x = \frac{F}{E_x} - \frac{2F\nu_\theta}{E_\theta} \tag{1}$$

$$\varepsilon_\theta = \frac{2F}{E_\theta} - \frac{F\nu_x}{E_x} \tag{2}$$

where E is the Young's modulus, ν is the Poisson ratio and the subscripts x and θ correspond to the longitudinal and circumferential directions, respectively. From our analysis, it is found that the intervals of the circumferential filaments in the apical region and those in the other regions are different. Therefore, in this analysis, it is assumed that the radius of the circumferential filaments is constant and that the number of the circumferential filaments in the apical region differs from that in the other regions, which leads to the difference between the circumferential Young's modulus in the apical region and that in the other regions; they are denoted by $E_{\theta a}$ and $E_{\theta o}$, respectively. On the other hand, as no difference in structure is noticeable in the longitudinal direction between the apical region and the other ones, the longitudinal Young's modulus is assumed

Table 2
Interval of the circumferential filaments in the middle region and in the other region

Region (from the basal end)	Mean (nm)	S.D. (nm)	Minimum (nm)	Maximum (nm)	Number of measurements	Number of OHCs
Between 0.0 and 0.4	54	18	18	103	126	4
Between 0.4 and 0.85	54	17	21	101	156	6

The mean interval of the circumferential filaments in the region between 0.0 and 0.4 from the basal end is the same as that in the region between 0.4 and 0.85 from the basal end.

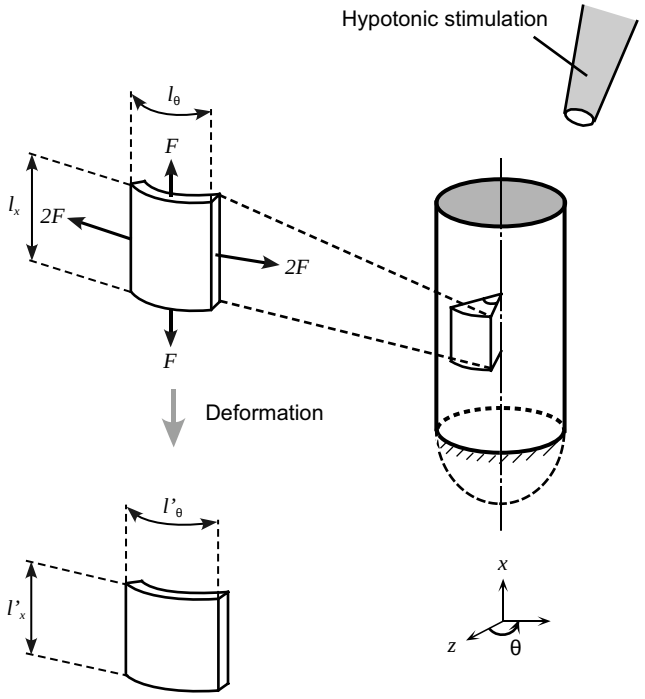

Fig. 8. Forces and strains of the cell lateral wall. When the OHC is perfused with hypotonic solution, the longitudinal force F and circumferential force $2F$ induced by an increase in the intracellular pressure act on the cell lateral wall. The longitudinal and circumferential lengths of the element, l_x and l_θ, are changed to l'_x and l'_θ, respectively, by these forces. Therefore, the longitudinal and circumferential strains of the cell lateral wall are obtained from $\varepsilon_x = (l'_x - l_x)/l_x$ and $\varepsilon_\theta = (l'_\theta - l_\theta)/l_\theta$, respectively.

to be constant. Owing to the orthotropism of the OHC lateral wall (Sugawara and Wada, 2001), the relationship between Young's modulus and Poisson's ratio of the OHC lateral wall in the apical region and that in the other regions are given by

$$\frac{E_{\theta a}}{E_x} = \frac{\nu_{\theta a}}{\nu_{xa}} = R_a \tag{3}$$

$$\frac{E_{\theta o}}{E_x} = \frac{\nu_{\theta o}}{\nu_{xo}} = R_o \tag{4}$$

where the subscripts a and o correspond to the apical and the other regions, respectively. Substituting Eqs. 3 and 4 into Eq. 1, one obtains the relationship between the longitudinal strain in the apical region and that in the other regions, which is expressed as follows:

$$\varepsilon_{xa} : \varepsilon_{xo} = \frac{F}{E_x} - \frac{2F\nu_{\theta a}}{E_{\theta a}} : \frac{F}{E_x} - \frac{2F\nu_{\theta o}}{E_{\theta o}} =$$

$$\frac{1}{E_{\theta a}}(R_a - 2\nu_{\theta a}) : \frac{1}{E_{\theta o}}(R_o - 2\nu_{\theta o}) \tag{5}$$

From the analysis of the OHC shell model, Sugawara and Wada (2001) found R to be 2.58 by comparing the numerical data and the experimental data of cell inflation (Iwasa and Chadwick, 1992) and axial stretch (Hallworth, 1995). In these experiments, bending moments are produced only near the cuticular plate, and the lateral wall of the OHC seems to be unaffected by bending moments. Therefore, the value of R obtained by Sugawara and Wada (2001) could be applied to R of the membrane model of this report in which bending moments are not taken into consideration. If R in the region between 0.0 and 0.85 from the basal end is assumed to be 2.58, Eq. 4 can be written as

$$\frac{E_{\theta o}}{E_x} = \frac{\nu_{\theta o}}{\nu_{xo}} = R_o = 2.58 \tag{6}$$

As the density of the circumferential filaments is high in the apical region of the cell, the circumferential Young's modulus of the cell lateral wall would be high in this region. The interval of the circumferential filaments in the apical region and that in the other regions are 44 nm and 54 nm, respectively. Therefore, the ratio of the circumferential Young's modulus of the cell lateral wall in the apical region to that in the other regions is assumed to be represented by

$$\frac{E_{\theta a}}{E_{\theta o}} = \frac{54}{44} \tag{7}$$

Inserting Eqs. 6 and 7 into Eq. 3 leads to

$$\frac{E_{\theta a}}{E_x} = \frac{\nu_{\theta a}}{\nu_{xa}} = R_a = 3.17 \tag{8}$$

Furthermore, as the value of $\varepsilon_x/\varepsilon_\theta$ obtained from a morphometric analysis of the changes in cell shape due to the hypotonic stimulation was -0.72 (Ratnanather et al., 1996), the ratio of the longitudinal strain to the circumferential one in the apical region and that in the other regions are assumed to be as follows:

$$\frac{\varepsilon_{xa}}{\varepsilon_{\theta a}} = \frac{\varepsilon_{xo}}{\varepsilon_{\theta o}} = -0.72 \tag{9}$$

Combining Eqs. 1, 2, 6, 8, and 9 yields

$$\nu_{\theta a} = 1.69 \tag{10}$$

$$\nu_{\theta o} = 1.48 \tag{11}$$

Substituting Eqs. 6, 7, 8, 10, and 11 into Eq. 5, the relationship between the longitudinal strain in the apical region and that in the other regions is given by

$$\varepsilon_{xa} : \varepsilon_{xo} = 0.45 : 1.0 \tag{12}$$

Therefore, it is expected that the longitudinal strain in the apical region of the cell is 45% of that in the other regions. These results indicate that the highly dense circumferential filaments in the apical region of the cell cause the high longitudinal stiffness in the apical region of the cell.

In our previous paper (Wada et al., 2001), when the

OHCs showed 5% shortening of the cell length due to hypotonic stimulation, the local deformation in the apical region of the cell was less than the analytical error (170 nm). As the mean OHC length used in the previous paper was 69.4 mm, 5% shortening of the cell length corresponded to 3.47 μm. When the deformation in the region between 0.881 and 1.0 from the basal end and the whole cell length change were 170 nm and 3.47 μm, respectively, the ratio of the longitudinal strain in the apical region of the cell to that in the other regions was obtained as follows:

$$\varepsilon_{xa} : \varepsilon_{xo} = \frac{170}{1.0-0.881} : \frac{3470-170}{0.881} = 0.38 : 1.0 \qquad (13)$$

Therefore, the longitudinal strain in the apical region of the cell is expected to be less than 38% of that in the other regions. As the experimental longitudinal strain in the apical region of the cell is smaller than 45% of the longitudinal strain in the other regions of the cell, in addition to the high density circumferential filaments, there must be other factors that cause the high stiffness in the apical region of the cell. One of these factors could be the cuticular plate which exists at the apical end of the cell and is composed of a dense network of actin filaments. Therefore, it would have a large influence on the circumferential Young's modulus in the apical region of the cell.

5. Conclusions

The ultrastructure of the OHC lateral wall was investigated by AFM. Then, the relationship between the ultrastructure and the local longitudinal stiffness along the cell axis, which was obtained by both analyzing the local deformation of the OHC in response to hypotonic stimulation and measuring the distribution of Young's modulus along the cell axis using the contact mode of the AFM, was examined. When the position along the cell axis is represented by the normalized distance from the basal end and the positions of the basal and apical ends are expressed by 0.0 and 1.0, the following conclusions can be drawn.

1. The circumferential filaments observed using tapping mode AFM appeared to be actins that are part of the cortical lattice.
2. The mean interval of the circumferential filaments in the region between 0.0 and 0.4 from the basal end and that in the region between 0.4 and 0.85 from the basal end were identical, namely, 54 nm. By contrast, the mean interval of the circumferential filaments in the region between 0.0 and 0.85 from the basal end and that in the region between 0.85 and 1.0 from the basal end were 54 nm and 44 nm, respectively.
3. The difference between the intervals of the circumferential filaments in the region between 0.0 and 0.85 and between 0.85 and 1.0 from the basal end was concluded to be one factor that causes the high stiffness in the apical region of the cell.

Acknowledgements

This research was supported by the Ministry of Education, Culture, Sports, Science and Technology of Japan under Grant-in-Aid for Scientific Research (A) No. 11307033.

References

Arima, T., Kuraoka, A., Toriya, R., Shibata, Y., Uemura, T., 1991. Quick-freeze, deep-etch visualization of the 'cytoskeletal spring' of cochlear outer hair cells. Cell Tissue Res. 263, 91–97.

Chang, L., Kious, T., Yorgancioglu, M., Keller, D., Pfeiffer, J., 1993. Cytoskeleton of living, unstained cells imaged by scanning force microscopy. Biophys. J. 64, 1282–1286.

Forge, A., 1991. Structural features of the lateral walls in mammalian cochlear outer hair cells. Cell Tissue Res. 265, 473–483.

Hallworth, R., 1995. Passive compliance and active force generation in the guinea pig outer hair cell. J. Neurophysiol. 74, 2319–2329.

Henderson, E., Haydon, P.G., Sakaguchi, D.S., 1992. Actin filament dynamics in living glial cells imaged by atomic force microscopy. Science 257, 1944–1946.

Holley, M.C., Ashmore, J.F., 1988. A cytoskeletal spring in cochlear outer hair cells. Nature 335, 635–637.

Holley, M.C., Ashmore, J.F., 1990a. Spectrin, actin and the structure of the cortical lattice in mammalian cochlear outer hair cells. J. Cell Sci. 96, 283–291.

Holley, M.C., Ashmore, J.F., 1990b. A cytoskeletal spring for the control of cell shape in outer hair cells isolated from the guinea pig cochlea. Eur. Arch. Otorhinolaryngol. 247, 4–7.

Holley, M.C., Kalinec, F., Kachar, B., 1992. Structure of the cortical cytoskeleton in mammalian outer hair cells. J. Cell Sci. 102, 569–580.

Huang, G., Santos-Sacchi, J., 1994. Motility voltage sensor of the outer hair cell resides within the lateral plasma membrane. Proc. Natl. Acad. Sci. USA 91, 12268–12272.

Iwasa, K.H., Chadwick, R.S., 1992. Elasticity and active force generation of cochlear outer hair cells. J. Acoust. Soc. Am. 92, 3169–3173.

Kalinec, F., Holley, M.C., Iwasa, K.H., Lim, D.J., Kachar, B., 1992. A membrane-based force generation mechanism in auditory sensory cells. Proc. Natl. Acad. Sci. USA 89, 8671–8675.

Leonova, E.V., Raphael, Y., 1999. Application of a platinum replica method to study of the cytoskeleton of isolated hair cells supporting cells and whole mounts of the organ of Corti. Hear. Res. 130, 137–154.

Ratnanather, J.T., Zhi, M., Brownell, W.E., 1996. The ratio of elastic moduli of cochlear outer hair cells derived from osmotic experiments. J. Acoust. Soc. Am. 99, 1025–1028.

Santos-Sacchi, J., 1991. Reversible inhibition of voltage-dependent outer hair cell motility and capacitance. J. Neurosci. 11, 3096–3110.

Slepecky, N., Ulfendahl, M., 1988. Glutaraldehyde induces cell shape

change in isolated outer hair cells from the inner ear. J. Submicrosc. Cytol. Pathol. 20, 37–45.
Sugawara, M., Wada, H., 2001. Analysis of elastic properties of outer hair cell wall using shell theory. Hear. Res. 160, 63–72.
Sugawara, M., Ishida, Y., Wada, H., 2002. Local mechanical properties of guinea pig outer hair cells measured by atomic force microscopy. Hear. Res. 174, 222–229.
Wada, H., Usukura, H., Takeuchi, S., Sugawara, M., Kakehata, S., Ikeda, K., 2001. Distribution of protein motors along the lateral wall of the outer hair cell. Hear. Res. 162, 10–18.
You, H.X., Lau, J.M., Zhang, S., Yu, L., 2000. Atomic force microscopy imaging of living cells: a preliminary study of the disruptive effect of the cantilever tip on cell morphology. Ultramicroscopy 82, 297–305.
Zenner, H.P., Gitter, A.H., Rudert, M., Ernst, A., 1992. Stiffness, compliance, elasticity and force generation of outer hair cells. Acta Otolaryngol. (Stockh.) 12, 248–253.
Zheng, J., Shen, W., He, D.Z.Z., Madison, L.D., Dallos, P., 2000. Prestin is the motor protein of cochlear outer hair cells. Nature 405, 149–155.